Ionospheric characteristics above Martian crustal magnetic anomalies

Paul Withers,[1] M. Mendillo,[1] H. Rishbeth,[1,2] D. P. Hinson,[3] and J. Arkani-Hamed[4]

[1] We studied several thousand electron density profiles from the Mars Global Surveyor Radio Science experiment. Electron densities in some of these profiles change significantly over vertical distances as short as $1-2$ km, often causing localized "bite-outs". These "anomalous" profiles are preferentially located above crustal magnetic anomalies. Anomalous features and their association with strong magnetic fields are also seen in profiles from Mariner 9. The probability of a profile being anomalous depends on the orientation of the magnetic field, suggesting localized electrodynamic effects upon otherwise global photochemical ionospheric processes. On Mars, unlike most other planets, the magnetic field has a short characteristic lengthscale, so its effects on the ionosphere will vary over short horizontal distances. We discuss possible ionospheric dynamo processes and encourage additional ionospheric observations over regions of strong crustal magnetic field. **Citation:** Withers, P., M. J. Mendillo, H. Rishbeth, D. P. Hinson, and J. Arkani-Hamed (2005), Ionospheric characteristics above Martian crustal magnetic anomalies, *Geophys. Res. Lett.*, *32*, L16204, doi:10.1029/2005GL023483.

1. Introduction

[2] The aims of this paper are (a) to describe some unusual vertical profiles of electron density in the ionosphere of Mars, (b) to correlate the spatial distribution of these profiles with magnetic field strength and direction, and (c) to discuss mechanisms by which the Martian magnetic field can affect the ionosphere.

[3] The Martian atmosphere is mostly CO_2. Its ionosphere, which displays Chapman-like photochemical behaviour and is dominated by O_2^+ ions, was compared to Earth's by *Mendillo et al.* [2003] and *Rishbeth and Mendillo* [2004]. The Martian magnetic field, formed by crustal sources, has a complex topology [*Acuña et al.*, 2001; *Lillis et al.*, 2004]. *Mitchell et al.* [2002] showed that the Martian ionopause is elevated by crustal magnetic fields. In a series of papers, *Krymskii et al.* [2004, and references therein] showed that the ionosphere is heated by the solar wind above crustal magnetic anomalies and that ionospheric scale heights are more variable in such regions. *Ness et al.* [2000] discovered that small amplitude, long wavelength oscillations in electron density were sometimes present between $200-250$ km over crustal magnetic anomalies, which they attributed to unsteady convection of ionospheric plasma along horizontal magnetic field lines. To date, numerical models of the effects of the magnetic field on the space environment at Mars have focused on the solar wind interaction rather than ionospheric processes such as conductivities and the ionospheric dynamo [e.g., *Ma et al.*, 2004].

[4] The Radio Science (RS) experiment on Mars Global Surveyor (MGS) has measured several thousand vertical profiles of ionospheric electron density at latitudes $60°N-86°N$ and 220 profiles at latitudes $64°S-70°S$ [*Hinson et al.*, 1999; *Tyler et al.*, 2001]. Typical profiles of electron density from the Northern and Southern hemispheres (NH and SH) are shown in Figure 1. Unusually large changes in electron density over a short vertical distance occur in some profiles from the SH, as shown in case 3 of Figure 1. These changes often lead to localized decreases in electron density ("bite-outs"), but can also lead to localized increases ("bumps"). Figure 2 shows several more examples. We tentatively label profiles containing such features as "anomalous". All data sets that yielded anomalous profiles were judged to be reliable, so these features appear to be associated with ionospheric structure rather than some sort of measurement error.

2. Definition and Distribution of Anomalous Profiles

[5] A profile consists of a series of electron densities, N_i, and uncertainties, σ_i, at heights z_i. We define the following quantities for each pair of adjacent data points, labelled i and $j = i + 1$, that are above 100 km and more than 2 km away from the ends of the profile: $z_{ij} = 0.5 \times (z_i + z_j)$, $\Delta z(z_{ij}) = z_i - z_j$, $\Delta N(z_{ij}) = N_i - N_j$, $s(z_{ij}) = (\sigma_i^2 + \sigma_j^2)^{1/2}$, and $A(z_{ij}) = |\Delta N(z_{ij})/\Delta z(z_{ij})|/N_{max}$, where N_{max} is the peak electron density. z_A is the height at which $A(z_{ij})$ equals its maximum value, A_{max}. If A_{max} exceeds a threshold value, A_0, and $|\Delta N|(z_A)/s(z_A)$ exceeds 1/2, then we consider a profile to be anomalous. An individual sample, x, from a normal distribution with mean μ and standard deviation σ has a 62% probability of satisfying $|x - \mu|/\sigma > 1/2$. $1/A_{max}$ has the dimensions of length and can be interpreted as the shortest lengthscale over which electron density changes significantly in a profile; we chose $1/A_0 = 6$ km. The mean of A_{max} for the 220 SH profiles was $(8.5 \text{ km})^{-1}$. Only 5 of 3529 (0.14%) profiles from the NH were classified as anomalous, whereas 20 of 220 (9.1%) profiles from the SH were. We shall concentrate on the SH data.

[6] The first of the 220 profiles in this series was measured on 6 May 1999, at 69.1°S, 12.2 hours local solar

[1]Center for Space Physics, Boston University, Boston, Massachusetts, USA.
[2]Permanently at School of Physics and Astronomy, University of Southampton, Southampton, UK.
[3]Department of Electrical Engineering, Stanford University, Stanford, California, USA.
[4]Department of Earth and Planetary Sciences, McGill University, Montreal, Quebec, Canada.
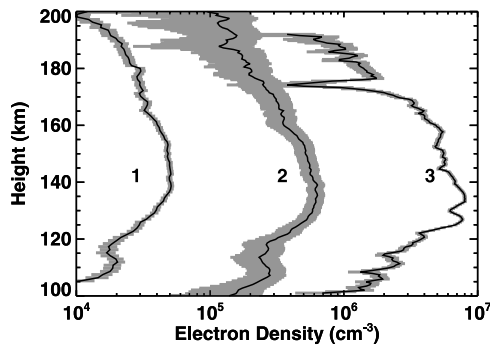
Figure 1. Three MGS RS electron density profiles. The profiles are marked by black lines and their 1σ uncertainties are marked by shaded regions. Case 1 is 0320A58A, a typical NH profile, case 2 is 9132I11A, a typical SH profile, and case 3 is 9149E12A, a SH profile with an anomalous feature. For display purposes, electron densities in case 1 have been multiplied by 1, those in case 2 by 10, and those in case 3 by 100.

[10] The probability that a given profile in a region of strong magnetic field is anomalous depends on both the azimuth, Az, and inclination, I, of the magnetic field. We use the absolute values of Az and I such that Az is between 0° and 180°, and I is between 0° and 90°. 23 profiles occur where $B > 100$ nT and $I < 30°$ at 150 km. 10 of the 23 occur where $45° < Az < 135°$, of which 1 is anomalous, whereas 6 of the 10 profiles outside this azimuthal range are anomalous. 41 profiles occur where $B > 100$ nT and $I > 30°$ at 150 km. 27 of the 41 occur where $45° < Az < 135°$, of which 7 are anomalous, whereas 2 of the 14 profiles outside this azimuthal range are anomalous. The azimuthal dependence may be related to the neutral wind or the geometry of the occultation. Numerical models predict south-eastward to southward winds of $\sim 100-200$ m s^{-1} at ionospheric heights and the latitude, season, and LST of these observations [*Bougher et al.*, 1999, 2000]. The MGS-Earth ray path direction changed monotonically from 11.7° to 25.5° west of north during the series of SH occultations.
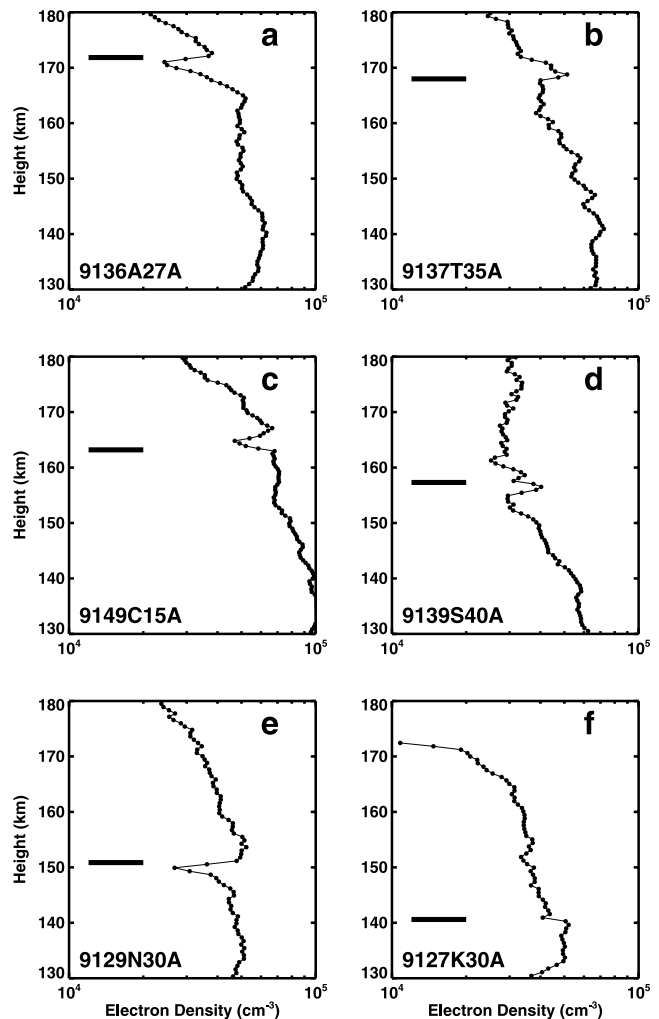
time (LST), 86.9° SZA, when Ls, the areocentric longitude of the Sun, was 135°. Latitude, LST, SZA, and Ls changed monotonically as additional profiles were acquired. The last profile was measured on 29 May 1999, at 64.7°S, 12.0 hours LST, 78.6° SZA, when Ls was 146°. Seventeen of the 20 anomalous profiles are at or above 138 km, the mean height of the peak electron density, and 3 are below.

[7] Figure 3 shows the spatial distribution of normal and anomalous profiles. Seventeen of the 43 (39.5%) profiles in the 130°–200°E longitude range are anomalous, whereas only 3 of the 177 (1.7%) profiles outside this range are anomalous. Of all the Martian properties that can affect the ionosphere, only the magnetic field has spatial structure consistent with this concentration in longitude and the rarity of NH anomalous profiles. Sixteen of the 20 anomalous profiles occur where the magnetic field exceeds 100 nT at 150 km. The magnetic field between 60°N and 86°N never exceeds this threshold.

[8] We visually examined electron density profiles from revolutions 1–79 of the Mariner 9 spacecraft (Figure 3) and concluded that 12 of them are potentially anomalous [*Zhang et al.*, 1990]. Revolution 22 is a particularly clear example. These potentially anomalous profiles also generally occur in regions of strong magnetic field. Anomalous features in Martian ionospheric profiles and their association with strong magnetic fields are real. A cursory examination of profiles from Venus does not show any anomalous features [*Brace et al.*, 1983; *Kliore*, 1992].

3. Anomalous Profiles and the Magnetic Field

[9] We use the magnetic field model of *Arkani-Hamed* [2004] up to degree and order 50, which has a spatial resolution (full wavelength) of 400–450 km and neglects the solar wind. An example fieldline, which is very different from terrestrial dipolar fieldlines, is shown in Figure 4. Thus, the horizontal scale of each RS profile, which is $\sim\sqrt{HR}$, where H is the scale height and R is the planetary radius, or ~ 200 km, is comparable to the horizontal scale of our magnetic field model [*Ness et al.*, 2000].

Figure 2. Six anomalous electron density profiles. Data points are marked by solid circles and linked by a thin solid line. Uncertainties, not shown, are similar to those in case 2 of Figure 1. The height of each anomalous feature is marked by a thick horizontal bar.

Modelling is required to determine the cause of this dependence on orientation.

4. Discussion of Ionospheric Dynamo Processes

[11] Much of the Martian ionosphere is in the photochemically-dominated regime, comparable to the terrestrial E-region which has interesting electrodynamics. The combination of strong winds, magnetic fields, and ionized plasma strongly suggests that dynamo action could produce electric currents on Mars. We here consider the effects of a Martian ionospheric dynamo in the magnetized regions of the ionosphere, especially those influenced by directional factors such as the neutral wind and anisotropic conductivity. The effects of magnetic fields are controlled by ν_{in}/ω_i and ν_{en}/ω_e, where ν_{in} and ν_{en} are the ion-neutral and electron-neutral collision frequencies, respectively, and ω_i and ω_e are the ion and electron gyrofrequencies. On Mars, the electron gyroradius ~ 4 m and the ion gyroradius ~ 1 km when $B = 100$ nT, as compared to the terrestrial E-region values of ~ 1 cm and ~ 30 m, respectively. Ionospheric conductivity is confined to the height range between h_i, where $\nu_{in}/\omega_i = 1$, and h_e, where $\nu_{en}/\omega_e = 1$, in which electrons are "frozen-in" to fieldlines but ions are not; the separation $h_i - h_e \sim H \ln (\nu_{in}\omega_e/\nu_{en}\omega_i)$, where H is the scale height [*Rishbeth and Garriott*, 1969].

[12] We use the atmospheric model in *Martinis et al.* [2003], $B = 100$ nT, O_2^+ ions, and expressions for collision frequencies from *Banks and Kockarts* [1973a, 1973b] and *Schunk and Nagy* [2000] to find that $h_e = 120$ km and $h_i = $

Figure 4. The thick white line shows the magnetic fieldline that passes through the height of the anomalous feature (150.5 km) in profile 9129N30A at the profile's latitude ($-68.6°$N) and longitude (165.6°E). Meridional and vertical projections of that fieldline are shown by green and pink lines, respectively. Electron densities (Ne) are shown by a black line in the meridional plane with a separate scale bar above. Uncertainties, not shown, are similar to those in case 2 of Figure 1.

190 km. Thus the anomalous features are observed at heights where the magnetic field affects ionospheric processes. On Earth, where the ionosphere spans ~ 1000 km, this "conducting layer" lies between 75 and 130 km at midlatitudes, mostly in the E-region, though the lower part is in the D-region where conductivity is negligible. By contrast, almost all of the Martian ionosphere is within this conducting layer when $B = 100$ nT.

[13] We assume that this layer has a uniform electron density $N = 3 \times 10^4$ cm^{-3} and scale height $H = 10$ km, and estimate conductivities, currents, and induced magnetic fields [*Rishbeth and Garriott*, 1969]. The Pedersen conductivity peaks at h_i and h_e with peak values $\sim Ne/2B$, thickness $\sim H$, and height-integrated value $\Sigma_1 \sim 2NeH/B = 1000$ mho, compared to 10 mho for the Earth where B is much greater and only the upper Pedersen peak at h_i contributes. The Hall conductivity is approximately Ne/B in a layer between h_e and h_i, so it has a height-integrated value $\Sigma_2 \sim (h_i - h_e) Ne/B = 3000$ mho, compared to 20 mho for the Earth. The direct conductivity, $Ne\omega_e/B\nu_{en}$, which increases exponentially upwards, already exceeds the Pedersen and Hall conductivities at h_e and may be treated as infinite above about $h_e + H$. A neutral wind, U, of 100 m s^{-1} induces an electric field $BU \sim 10$ μV m^{-1}, which drives a Hall current of $\Sigma_2 BU \sim 30$ A km^{-1}, which in turn induces a magnetic field of $(Ne/B) BU\mu_0 (h_i - h_e) \sim 40$ nT. These values are greater than the terrestrial values of ~ 10 A km^{-1} and ~ 10 nT. The induced field is almost comparable to the assumed magnetic field strength of 100 nT. Thus, Martian ionospheric currents may significantly modify the magnetic field that produces them.

[14] When the Martian magnetic field is horizontal, an "equatorial electrojet" may be present. On Earth, the
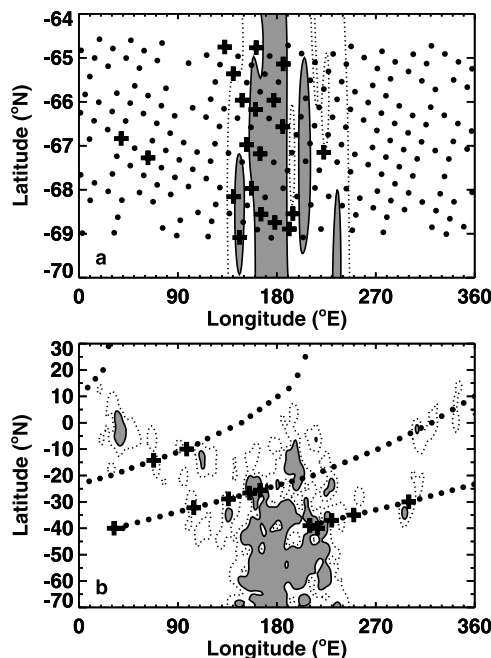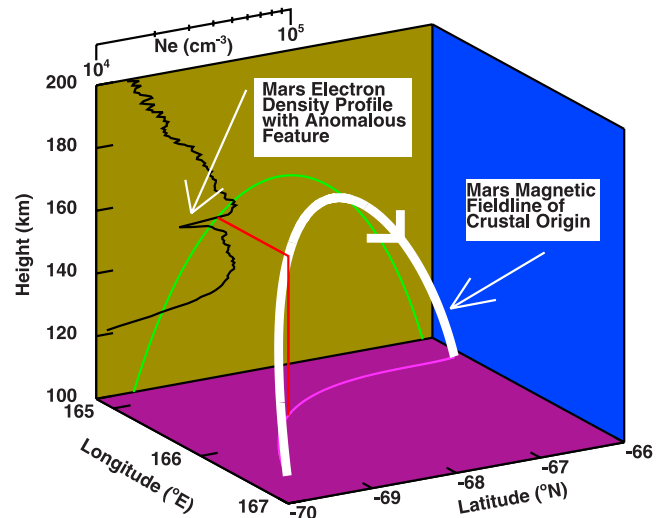

Figure 3. (a) Anomalous MGS ionospheric profiles (pluses) and normal profiles (dots) from the Southern Hemisphere in 1999. The magnetic field at 150 km is shown by dotted contours at 100 nT and solid contours at 200 nT. Regions where the magnetic field is stronger than 200 nT are shaded. (b) As Figure 3a, but showing profiles from revolutions 1–79 of Mariner 9 in 1971–1972 [*Kliore*, 1974; *Zhang et al.*, 1990]. Profiles from revolutions 2, 3, 4, 8, 12, 19, 22, 25, 29, 31, 48, and 54 appear to be anomalous.

equatorial ionosphere exhibits complex plasma instability phenomena, especially around sunset. These Martian ionospheric profiles have SZAs between 78° and 87°, so it is possible that the anomalous Martian profiles are displaying similar phenomena associated with the strong day/night gradient of conductivity.

5. Conclusions

[15] We have developed a quantitative and reproducible way of identifying ionospheric profiles that have large changes in electron density over vertical distances as short as 1−2 km, which we label "anomalous. We have applied this technique to several thousand ionospheric profiles from the MGS RS experiment, of which 25 are anomalous.

[16] Anomalous profiles are most likely to occur in regions where the magnetic field is strong, implying an association between the field, which affects plasma transport, and the anomalous features. The anomalous features could represent sharp vertical changes in electron density, or horizontal changes, or both. In either case, the change must be quite abrupt, with a characteristic spatial scale of a few kilometres or less. Modelling of plasma transport in the Martian magnetic field is needed to determine the cause of anomalous features. The assumptions inherent in the data inversion technique should also be considered. It seems likely that the unique nature of the Martian magnetic field will lead to phenomena not seen at Earth, such as localized dynamo regions and local variations in transport processes.

[17] There have been no ionospheric measurements over Southern Hemisphere magnetic anomalies by MGS since these 220 profiles from May 1999. Future ionospheric measurements over crustal magnetic anomalies may be made by the Mars Express Radio Science and MARSIS instruments, as well as the MGS RS experiment. We encourage such measurements. Re-examination of digital datasets from Mariner 9 and Viking Orbiters 1 and 2, if available, would also be worthwhile.

References

Acuña, M. H., et al. (2001), Magnetic field of Mars: Summary of results from the aerobraking and mapping orbits, *J. Geophys. Res.*, *106*, 23,403–23,418.

Arkani-Hamed, J. (2004), A coherent model of the crustal magnetic field of Mars, *J. Geophys. Res.*, *109*, E09005, doi:10.1029/2004JE002265.

Banks, P. M., and G. Kockarts (1973a), Collision processes, in *Aeronomy, Part A*, chap. 9, pp. 184–239, Elsevier, New York.

Banks, P. M., and G. Kockarts (1973b), Plasma transport, in *Aeronomy, Part B*, chap. 19, pp. 152–168, Elsevier, New York.

Bougher, S. W., S. Engel, R. G. Roble, and B. Foster (1999), Comparative terrestrial planet thermospheres: 2. Solar cycle variation of global structure and winds at equinox, *J. Geophys. Res.*, *104*, 16,591–16,611.

Bougher, S. W., S. Engel, R. G. Roble, and B. Foster (2000), Comparative terrestrial planet thermospheres: 3. Solar cycle variation of global structure and winds at solstices, *J. Geophys. Res.*, *105*, 17,669–17,692.

Brace, L. H., H. A. Taylor, T. I. Gombosi, A. J. Kliore, W. C. Knudsen, and A. F. Nagy (1983), The ionosphere of Venus: Observations and their interpretations, in *Venus*, edited by D. M. Hunten et al., pp. 779–840, Univ. of Arizona Press, Tucson.

Hinson, D. P., R. A. Simpson, J. D. Twicken, G. L. Tyler, and F. M. Flasar (1999), Initial results from radio occultation measurements with Mars Global Surveyor, *J. Geophys. Res.*, *104*, 26,997–27,012.

Kliore, A. J. (1974), Radio occultation exploration of Mars, in *Exploration of the Planetary System*, IAU Symp. Ser., vol. 65, edited by A. Woszczyk and C. Iwaniszewska, pp. 295–316, Springer, New York.

Kliore, A. J. (1992), Radio occultation observations of the ionospheres of Mars and Venus, in *Venus and Mars: Atmospheres, Ionospheres, and Solar Wind Interactions*, Geophys. Monogr. Ser., vol. 66, edited by J. G. Luhmann, M. Tatrallyay, and R. O. Pepin, pp. 265–276, AGU, Washington, D. C.

Krymskii, A. M., N. F. Ness, D. H. Crider, T. K. Breus, M. H. Acuña, and D. P. Hinson (2004), Solar wind interaction with the ionosphere/atmosphere and crustal magnetic fields at Mars: Mars Global Surveyor Magnetometer/Electron Reflectometer, radio science and accelerometer data, *J. Geophys. Res.*, *109*, A11306, doi:10.1029/2004JA010420.

Lillis, R. J., D. L. Mitchell, R. P. Lin, J. E. P. Connerney, and M. H. Acuña (2004), Mapping crustal magnetic fields at Mars using electron reflectometry, *Geophys. Res. Lett.*, *31*, L15702, doi:10.1029/2004GL020189.

Ma, Y., A. F. Nagy, I. V. Sokolov, and K. C. Hansen (2004), Three-dimensional, multispecies, high spatial resolution MHD studies of the solar wind interaction with Mars, *J. Geophys. Res.*, *109*, A07211, doi:10.1029/2003JA010367.

Martinis, C. R., J. K. Wilson, and M. J. Mendillo (2003), Modeling day-to-day ionospheric variability on Mars, *J. Geophys. Res.*, *108*(A10), 1383, doi:10.1029/2003JA009973.

Mendillo, M., S. Smith, J. Wroten, H. Rishbeth, and D. P. Hinson (2003), Simultaneous ionospheric variability on Earth and Mars, *J. Geophys. Res.*, *108*(A12), 1432, doi:10.1029/2003JA009961.

Mitchell, D. L., R. P. Lin, H. Reme, P. A. Cloutier, J. E. P. Connerney, M. H. Acuña, and N. F. Ness (2002), Probing Mars' crustal magnetic field and ionosphere with the MGS Electron Reflectometer, *Lunar Planet. Sci.* [CD-ROM], *XXXIII*, Abstract 2029.

Ness, N. F., M. H. Acuña, J. E. P. Connerney, A. J. Kliore, T. K. Breus, A. M. Krymskii, P. Cloutier, and S. J. Bauer (2000), Effects of magnetic anomalies discovered at Mars on the structure of the Martian ionosphere and solar wind interaction as follows from radio occultation experiments, *J. Geophys. Res.*, *105*, 15,991–16,004.

Rishbeth, H., and O. K. Garriott (1969), Transport processes in the ionosphere, in *Introduction to Ionospheric Physics*, chap. 4, pp. 126–159, Elsevier, New York.

Rishbeth, H., and M. Mendillo (2004), Ionospheric layers of Earth and Mars, *Planet. Space Sci.*, *52*, 849–852.

Schunk, R. W., and A. F. Nagy (2000), Collisions, in *Ionospheres*, chap. 4, pp. 66–103, Cambridge Univ. Press, New York.

Tyler, G. L., G. Balmino, D. P. Hinson, W. L. Sjogren, D. E. Smith, R. A. Simpson, S. W. Asmar, P. Priest, and J. D. Twicken (2001), Radio science observations with Mars Global Surveyor: Orbit insertion through one Mars year in mapping orbit, *J. Geophys. Res.*, *106*, 23,327–23,348.

Zhang, M. H. G., J. G. Luhmann, A. J. Kliore, and J. Kim (1990), A post-Pioneer Venus reassessment of the Martian dayside ionosphere as observed by radio occultation methods, *J. Geophys. Res.*, *95*, 14,829–14,839.

_____

J. Arkani-Hamed, Earth and Planetary Sciences, 3450 University St., Montreal, QC, Canada H3A 2A7.

D. P. Hinson, Department of Electrical Engineering, Stanford University, Stanford, CA 94305, USA.

M. Mendillo and P. Withers, Center for Space Physics, Boston University, 725 Commonwealth Avenue, Boston, MA 02215, USA. (withers@bu.edu)

H. Rishbeth, School of Physics and Astronomy, University of Southampton, Highfield, Southampton SO17 1BJ, UK.